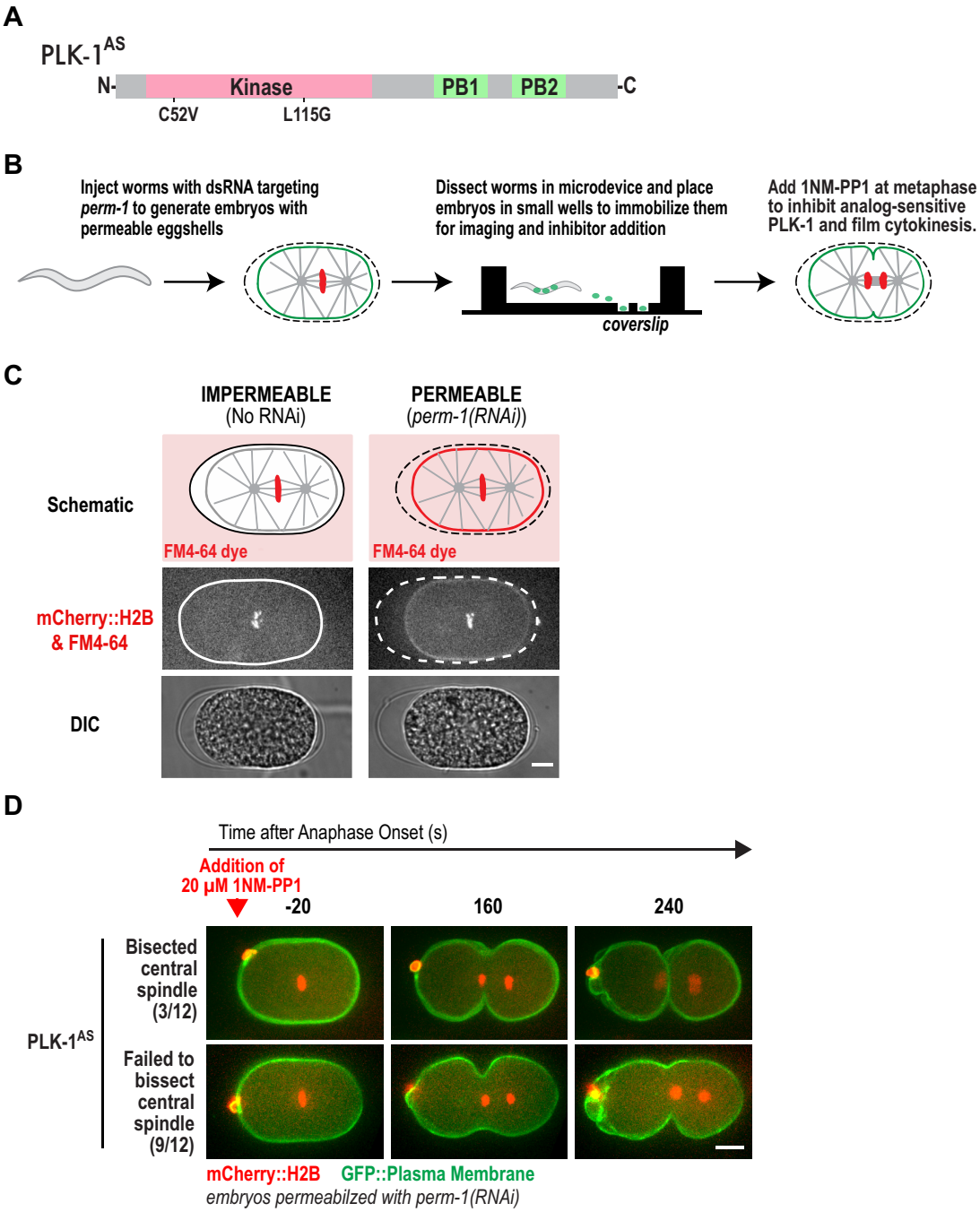
A
PLK-1AS
N-
Kinase
PB1
PB2
-C
C52V
L115G
B
Inject worms with dsRNA targeting perm-1 to generate embryos with permeable eggshells
Dissect worms in microdevice and place embryos in small wells to immobilize them for imaging and inhibitor addition
Add 1NM-PP1 at metaphase to inhibit analog-sensitive PLK-1 and film cytokinesis.
coverslip
C
IMPERMEABLE
(No RNAi)
PERMEABLE
(perm-1(RNAi))
Schematic
FM4-64 dye
FM4-64 dye
mCherry::H2B & FM4-64
DIC
D
Time after Anaphase Onset (s)
Addition of 20 µM 1NM-PP1
-20
160
240
PLK-1AS
Bisected central spindle (3/12)
Failed to bisect central spindle (9/12)
mCherry::H2B
GFP::Plasma Membrane
embryos permeabilzed with perm-1(RNAi)

Figure S1. Outline of experiment to analyze the effect of acute inhibition of PLK-1 kinase activity on cytokinesis, Related to Figure 1. (**A**) Schematic shows the location of the amino acid changes (C52V and L115G) introduced via CRISPR/Cas9 editing into the endogenous *plk-1* locus to generate worms expressing the analog-sensitive protein (PLK-1AS). (**B**) Schematic outline of the procedure used to inhibit PLK-1AS during cytokinesis in 1-cell stage *C. elegans* embryos. (**C**) Schematics and single-plane images of impermeable (*left*, No RNAi) and permeable (*right*, *perm-1(RNAi)*) embryos co-expressing mCherry::H2B and a GFP-tagged plasma membrane marker (not shown). Embryos were exposed to media containing lipophilic dye FM4-64 (*red*), which labels the plasma membrane of permeable, but not impermeable embryos. Scale bar, 10 μm. (**D**) Images from timelapse movies of permeabilized one-cell embryos expressing analog-sensitive (AS) PLK-1 and the indicated fluorescent markers taken from the experiment described in Figure 1 B,C. 1-NM-PP1, which inhibits analog-sensitive PLK-1, was added at metaphase (*red arrowhead*). In 9 out of 12 1NM-PP1-treated PLK-1AS embryos, the cleavage furrow initially failed to bisect the central spindle (*bottom row);* in 3 of these cases misalignment was ultimately rescued to allow cytokinesis completion, and in the remaining 6 cases cytokinesis failed. In contrast to 1NM-PP1-treated PLK-1AS embryos (**Figure 1B**), the NOP-1-dependent furrows in CYK-4 4A and Δ163-180 mutant embryos (**Figure 3C**) did not exhibit this phenotype were aligned with the midpoint between the chromosomes. We suspect that this difference arises because PLK-1 inhibition affects astral microtubules by promoting disassembly of the mitotic PCM [S1], as well as preventing the central spindle from generating CYK-4 phosphorylated on its N-terminal PLK-1 target site cluster, thus simultaneously compromising two key furrow positioning mechanisms. Scale bar, 10 μm.

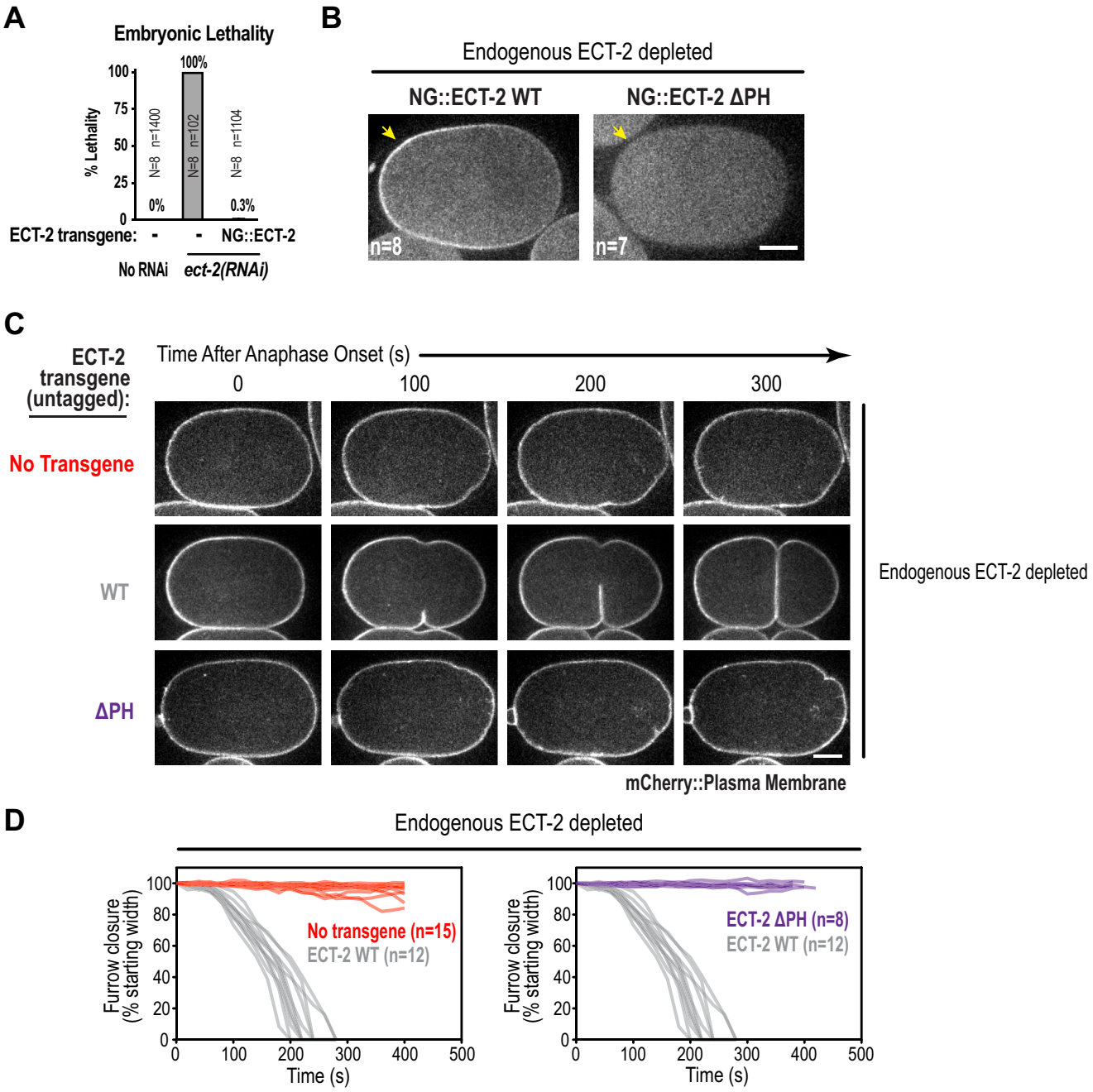
A
Embryonic Lethality
% Lethality
100
75
50
25
0
N=8 n=1400
N=8 n=102
N=8 n=1104
0%
100%
0.3%
ECT-2 transgene: - - NG::ECT-2
No RNAi
ect-2(RNAi)
B
Endogenous ECT-2 depleted
NG::ECT-2 WT
NG::ECT-2 ΔPH
n=8
n=7
C
ECT-2 transgene (untagged):
Time After Anaphase Onset (s)
0
100
200
300
No Transgene
WT
ΔPH
Endogenous ECT-2 depleted
mCherry::Plasma Membrane
D
Endogenous ECT-2 depleted
Furrow closure (% starting width)
No transgene (n=15)
ECT-2 WT (n=12)
Time (s)
ECT-2 ΔPH (n=8)
ECT-2 WT (n=12)
Time (s)

Figure S2. The ECT-2 PH domain is required for localization to the plasma membrane and for ECT-2 function in RhoA activation, Related to Figure 2. (**A**) Graph plots percent embryonic lethality (mean ± SD) in control embryos or after depletion of endogenous ECT-2 from embryos without an ECT-2 transgene or expressing NG::ECT-2 from an RNAi-resistant transgene. N is number of worms; n is the number of embryos scored per condition. (**B**) Fluorescence confocal images of embryos expressing transgene-encoded WT NG::ECT-2 or a NeonGreen fusion with ECT-2 lacking its C-terminal pleckstrin homology (PH) domain. Deletion of the PH domain abrogates targeting to the plasma membrane. (**C**) Single central plane confocal images of the cell equator from time-lapse sequences of embryos expressing an mCherry::plasma membrane marker that were depleted of endogenous ECT-2. Sequences are shown for representative embryos either lacking an ECT-2 transgene (n=15) or reconstituted with transgenes expressing untagged WT ECT-2 (n=12) or the ECT-2 ΔPH mutant (n=8) that cannot localize to the plasma membrane. Series begin at anaphase onset. Scale bar, 10μm. (**D**) Graphs showing the kinetics of contractile ring closure in individual embryos for the conditions shown in (C). The set of traces of embryos expressing WT ECT-2 are the control and are shown in gray on all both graphs.

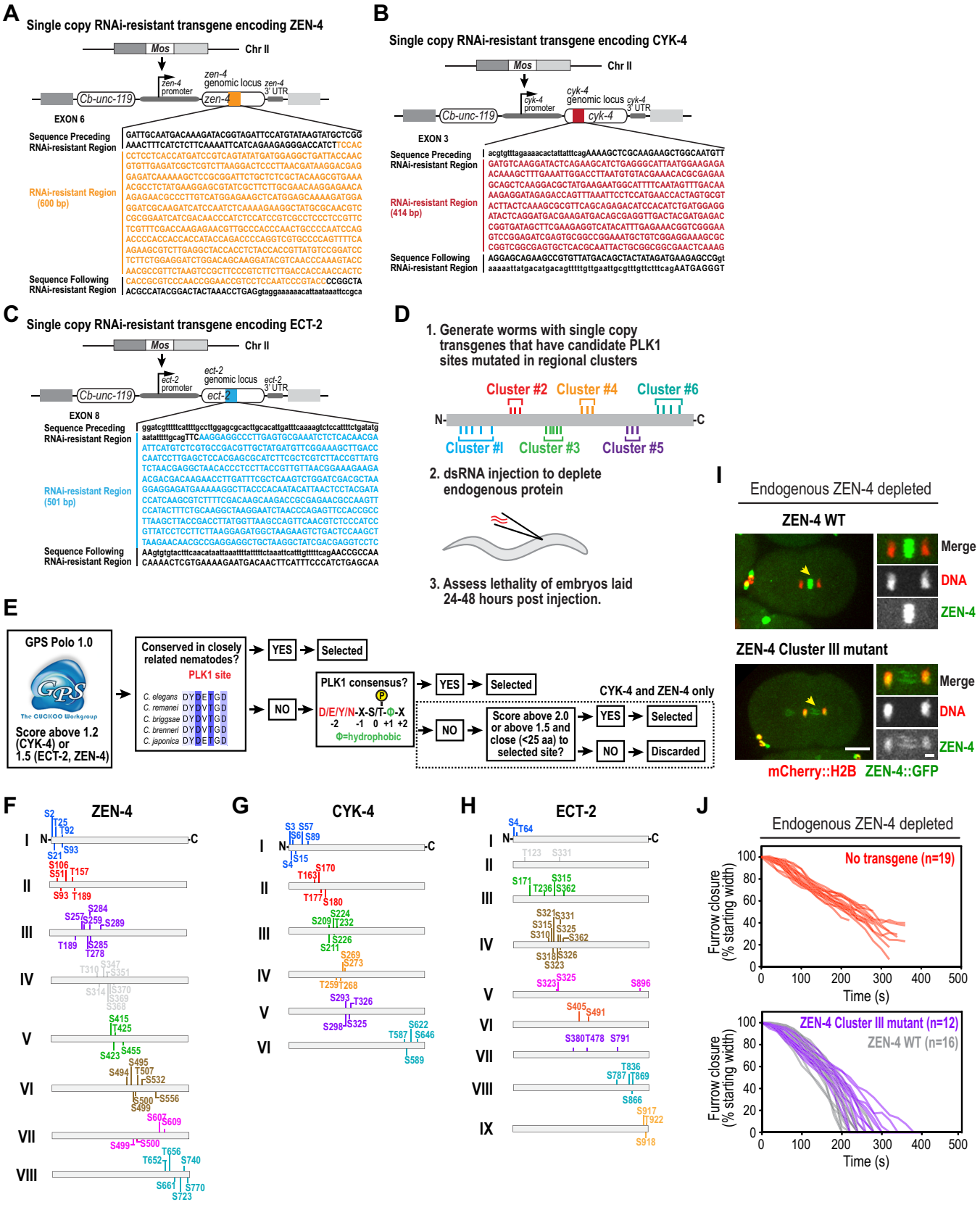
A
Single copy RNAi-resistant transgene encoding ZEN-4
Mos
Chr II
zen-4 promoter
zen-4 genomic locus
zen-4 3' UTR
Cb-unc-119
zen-4
EXON 6
Sequence Preceding RNAi-resistant Region
RNAi-resistant Region (600 bp)
Sequence Following RNAi-resistant Region
B
Single copy RNAi-resistant transgene encoding CYK-4
cyk-4 promoter
cyk-4 genomic locus
cyk-4 3' UTR
EXON 3
RNAi-resistant Region (414 bp)
C
Single copy RNAi-resistant transgene encoding ECT-2
ect-2 promoter
ect-2 genomic locus
ect-2 3' UTR
EXON 8
RNAi-resistant Region (501 bp)
D
1. Generate worms with single copy transgenes that have candidate PLK1 sites mutated in regional clusters
Cluster #2
Cluster #4
Cluster #6
Cluster #1
Cluster #3
Cluster #5
2. dsRNA injection to deplete endogenous protein
3. Assess lethality of embryos laid 24-48 hours post injection.
E
GPS Polo 1.0
The CUCKOO Workgroup
Score above 1.2 (CYK-4) or 1.5 (ECT-2, ZEN-4)
Conserved in closely related nematodes?
PLK1 site
C. elegans DYDETGD
C. remanei DYDVTGD
C. briggsae DYDVTGD
C. brenneri DYDVTGD
C. japonica DYDETGD
YES
Selected
NO
PLK1 consensus?
D/E/Y/N-X-S/T-Φ-X
-2 -1 0 +1 +2
Φ=hydrophobic
CYK-4 and ZEN-4 only
Score above 2.0 or above 1.5 and close (<25 aa) to selected site?
Discarded
F
ZEN-4
G
CYK-4
H
ECT-2
I
Endogenous ZEN-4 depleted
ZEN-4 WT
Merge
DNA
ZEN-4
ZEN-4 Cluster III mutant
mCherry::H2B ZEN-4::GFP
J
Endogenous ZEN-4 depleted
No transgene (n=19)
Furrow closure (% starting width)
Time (s)
ZEN-4 Cluster III mutant (n=12)
ZEN-4 WT (n=16)

Figure S3. Construction of ZEN-4, CYK-4 and ECT-2 transgenes for regional mutagenesis of candidate PLK-1 sites, Related to Figure 2. (A-C) Schematics of the single-copy transgenes encoding ZEN-4, CYK-4 and ECT-2 inserted into a specific locus on chromosome II. *Cb unc-119*, the *unc-119* coding region from the related nematode *C. briggsae*, was used as a transformation marker. Transgenes were re-encoded while maintaining amino acid sequence across the indicated region to render them resistant to RNAi targeting the endogenous gene. (**D**) Summary of the screening method used to test the functionality of mutants in clusters of candidate PLK-1 sites in ZEN-4, CYK-4 and ECT-2. (**E**) Algorithm used for the selection of candidate PLK-1 phosphorylation sites in ZEN-4, CYK-4 and ECT-2. (**F-H**) Schematics show each of the proteins encoded by the mutant transgenes, with the mutated residues in each cluster listed, for ZEN-4 (F), CYK-4 (G), and ECT-2 (H). (**I**) Fluorescence confocal images from time lapse series of embryos expressing WT (*top*) or cluster III mutant (*bottom*) ZEN-4::GFP along with H2B::mCherry after depletion of endogenous ZEN-4 by RNAi. Images were acquired 100 seconds after anaphase onset. Panels to the right show a higher magnification view of the central spindle. Scale bars, 10 μm (main), 2μm (higher magnification panels). (**J**) Graphs show traces of furrow width versus time for individual embryos from the indicated conditions expressing an mCherry-tagged plasma membrane probe.

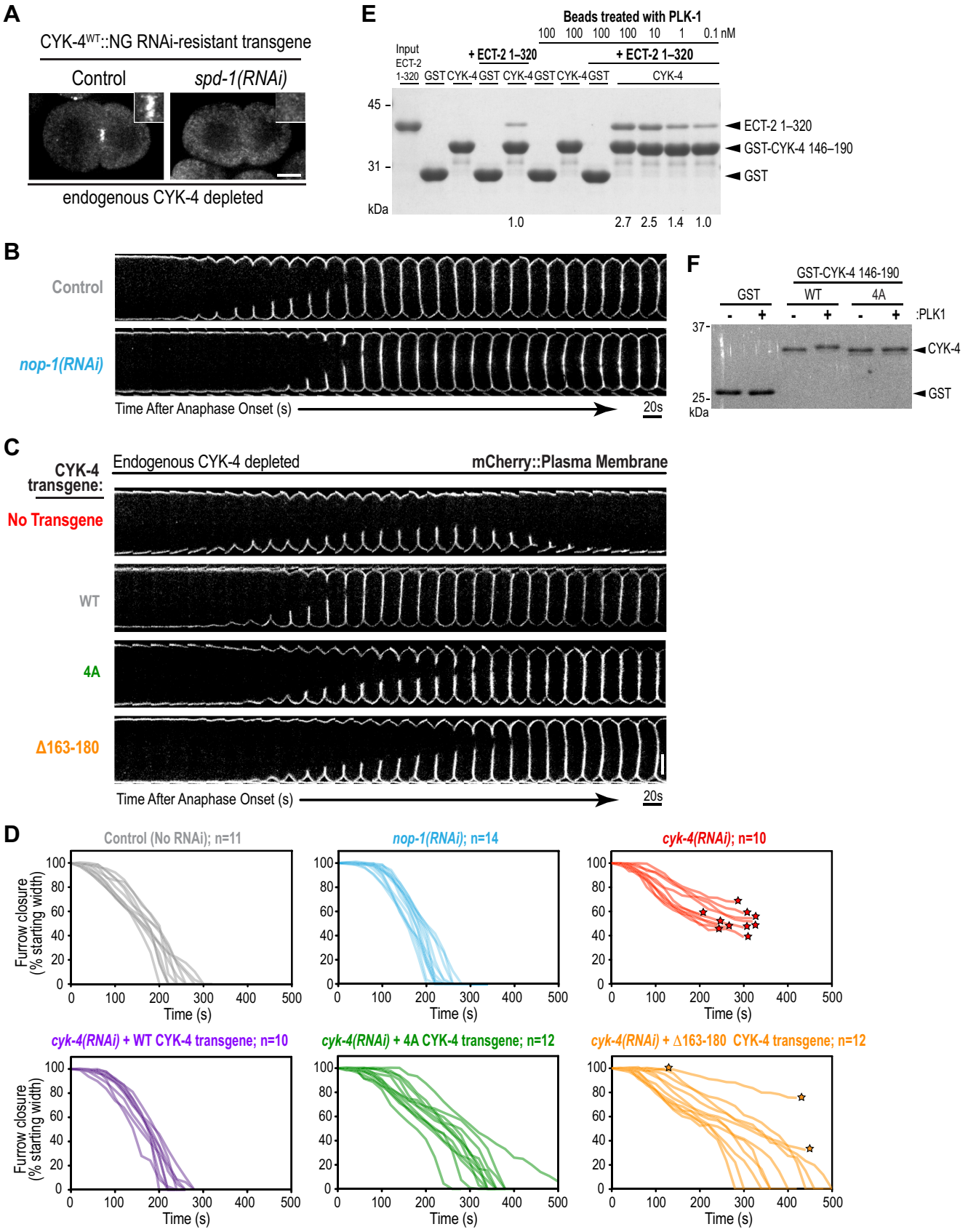
A
CYK-4WT::NG RNAi-resistant transgene
Control
spd-1(RNAi)
endogenous CYK-4 depleted
E
Beads treated with PLK-1
100 100 100 100 10 1 0.1 nM
Input ECT-2 1-320
+ ECT-2 1–320
+ ECT-2 1–320
GST CYK-4 GST CYK-4 GST CYK-4 GST CYK-4
45
31
kDa
ECT-2 1–320
GST-CYK-4 146–190
GST
1.0
2.7 2.5 1.4 1.0
B
Control
nop-1(RNAi)
Time After Anaphase Onset (s)
20s
F
GST-CYK-4 146-190
GST
WT
4A
- + - + - + :PLK1
37
25
kDa
CYK-4
GST
C
CYK-4 transgene:
Endogenous CYK-4 depleted
mCherry::Plasma Membrane
No Transgene
WT
4A
Δ163-180
Time After Anaphase Onset (s)
20s
D
Control (No RNAi); n=11
nop-1(RNAi); n=14
cyk-4(RNAi); n=10
cyk-4(RNAi) + WT CYK-4 transgene; n=10
cyk-4(RNAi) + 4A CYK-4 transgene; n=12
cyk-4(RNAi) + Δ163-180 CYK-4 transgene; n=12
Furrow closure (% starting width)
Time (s)

Figure S4. Phenotypes of the CYK-4 PLK-1 phosphorylation site mutants in the presence of the *C. elegans*-specific RhoA activator NOP-1, Related to Figure 3. (**A**) Representative images of embryos expressing CYK-4::NG WT either without or with depletion of endogenous SPD-1 by RNAi. The control embryo without depletion is repeated from Figure 3B for comparison. Images were acquired 200 seconds after anaphase onset. Insets are magnified 3X. Scale bar, 10μm. (**B, C**) Single central plane confocal images of the cell equator from time-lapse sequences of embryos expressing an mCherry::plasma membrane marker. (**B**) Image sequences show a representative control embryo (No RNAi; n=11) and an embryo depleted of NOP-1 (*nop-1(RNAi)*; n=14). (**C**) Image sequences show representative embryos in which endogenous CYK-4 has been depleted and reconstituted with no CYK-4 transgene (n=10) or with transgenes expressing untagged WT (n=10), or 4A (n=12) or Δ163-180 (n=12) mutant CYK-4. Series begin at anaphase onset. Scale bar, 10 μm. (**D**) Graphs showing the kinetics of contractile ring closure in individual embryos for the conditions shown in (B and C). Stars mark the final furrow width before regression. (**E**) Gel showing the effects of reducing PLK-1 levels on the ability of GST-CYK-4 146–190 beads to pull down ECT-2 1–320. GST-CYK-4 146–190 beads were treated with the indicated concentrations of PLK-1 T194D (0.1–100 nM), before washing the beads to remove PLK-1 and mixing with ECT-2 1–320 in the pulldown experiment. Pulldown results were analyzed by SDS-PAGE and Coomassie staining. 100 nM PLK-1 resulted in the most significant upshift of the CYK-4 band, suggesting the most effective phosphorylation. Hence, PLK-1 was used at 100 nM in all subsequent pull-down experiments. Numbers below the lanes are quantification of the amount of ECT-2 1-320 pulled down relative to the amount pulled down by the WT CYK-4 fragment without pre-incubation with PLK-1. (**F**) Coomassie-stained gel showing that the migration of a GST fusion with WT CYK-4 146-190 decreases after incubation with PLK-1 kinase, suggesting phosphorylation, whereas the migration of GST fused to the same region of CYK-4 with the 4 candidate PLK-1 sites mutated to alanine (4A) does not.

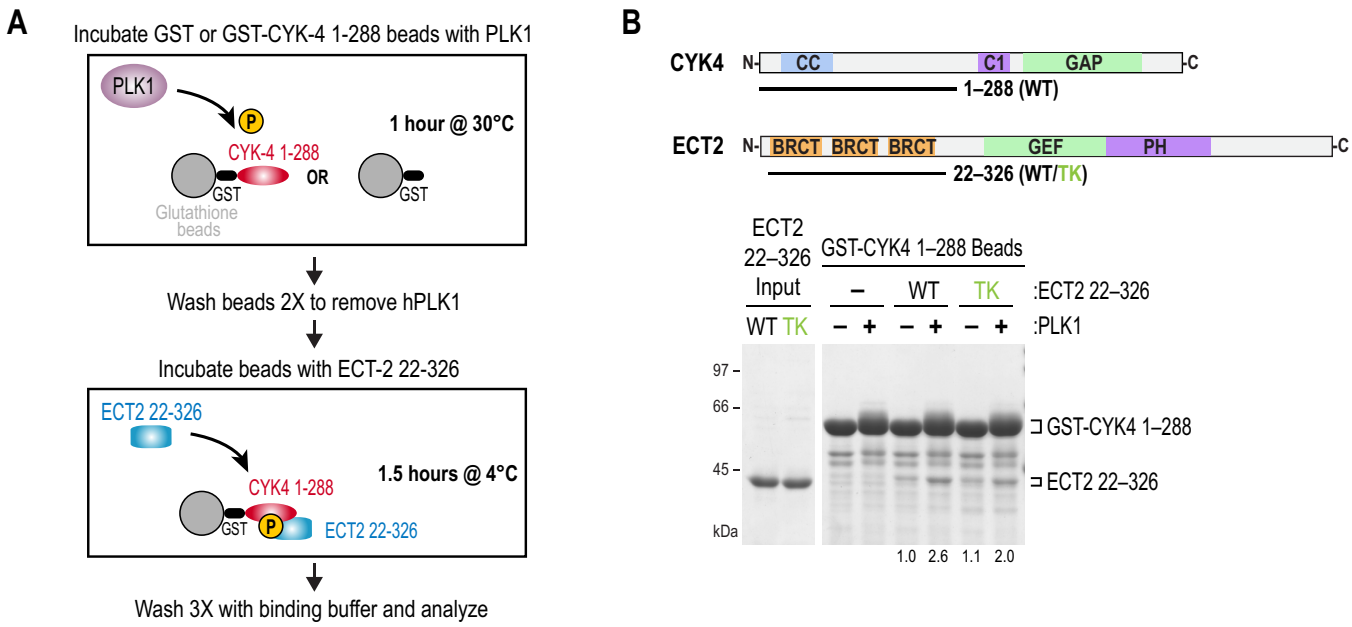

Figure S5. Mutation of canonical phospho-recognition residues in the BRCT module of human ECT2 does not affect binding to the N-terminus of human CYK-4, Related to Figure 4. A) Schematics illustrating the protocol for the kinase and pulldown assays to test the effect of PLK1 phosphorylation on the binding of the N-terminus of human CYK4 to ECT2. (**B**) *(top)* Schematics of human CYK4 1–288 and ECT2 22–326 (WT or TK mutant) proteins used in the pulldown assay. *(bottom)* Pulldown results analyzed by SDS-PAGE and Coomassie staining. Numbers below the lanes are quantification of the amount of ECT2 22-326 pulled down relative to the amount pulled down by WT CYK4 1-288 without pre-incubation with PLK1.

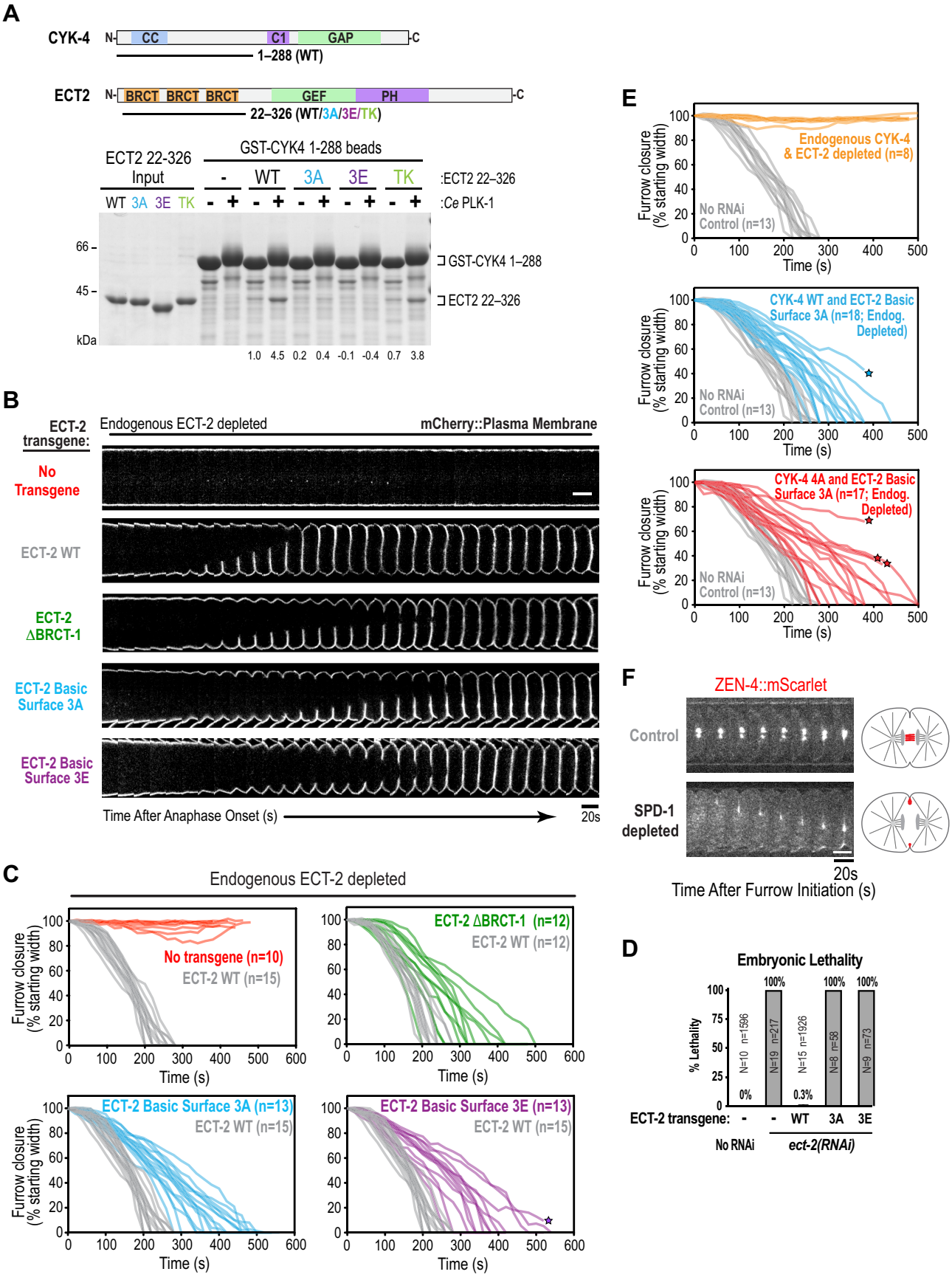
A
CYK-4
N-
CC
C1
GAP
-C
1–288 (WT)
ECT2
N-
BRCT BRCT BRCT
GEF
PH
-C
22–326 (WT/3A/3E/TK)
ECT2 22-326 Input
GST-CYK4 1-288 beads
-
WT
3A
3E
TK
:ECT2 22–326
:Ce PLK-1
WT 3A 3E TK
66
45
kDa
GST-CYK4 1–288
ECT2 22–326
1.0 4.5 0.2 0.4 -0.1 -0.4 0.7 3.8
B
ECT-2 transgene:
Endogenous ECT-2 depleted
mCherry::Plasma Membrane
No Transgene
ECT-2 WT
ECT-2 ΔBRCT-1
ECT-2 Basic Surface 3A
ECT-2 Basic Surface 3E
Time After Anaphase Onset (s)
20s
C
Endogenous ECT-2 depleted
Furrow closure (% starting width)
Time (s)
No transgene (n=10)
ECT-2 WT (n=15)
ECT-2 ΔBRCT-1 (n=12)
ECT-2 WT (n=12)
ECT-2 Basic Surface 3A (n=13)
ECT-2 WT (n=15)
ECT-2 Basic Surface 3E (n=13)
ECT-2 WT (n=15)
E
Furrow closure (% starting width)
Time (s)
Endogenous CYK-4 & ECT-2 depleted (n=8)
No RNAi Control (n=13)
CYK-4 WT and ECT-2 Basic Surface 3A (n=18; Endog. Depleted)
No RNAi Control (n=13)
CYK-4 4A and ECT-2 Basic Surface 3A (n=17; Endog. Depleted)
No RNAi Control (n=13)
F
ZEN-4::mScarlet
Control
SPD-1 depleted
20s
Time After Furrow Initiation (s)
D
Embryonic Lethality
% Lethality
0%
0.3%
100%
N=10 n=1596
N=19 n=217
N=15 n=1926
N=8 n=58
N=9 n=73
ECT-2 transgene: - - WT 3A 3E
No RNAi
ect-2(RNAi)

Figure S6. NOP-1 activates ECT-2 via a mechanism that does not require the ECT-2 basic surface, Related to Figure 5. (**A**) *(top)* Schematics of human CYK4 1–288 and ECT2 22–326 (WT or 3A, 3E or TK mutant) proteins used in the pulldown assay. *(bottom)* Pulldown results analyzed by SDS-PAGE and Coomassie staining. Numbers below the lanes are quantification of the amount of hECT2 22-326 pulled down relative to the amount pulled down by WT hCYK4 1-288 without pre-incubation with *C. elegans* PLK-1. (**B**) Single central plane confocal images of the cell equator from time-lapse sequences of embryos expressing an mCherry::plasma membrane marker in which endogenous ECT-2 has been depleted. Sequences are shown for representative embryos either lacking an ECT-2 transgene or reconstituted with transgenes expressing untagged WT ECT-2, ECT-2 with the BRCT-1 domain deleted, or the ECT-2 Basic Surface 3A or 3E mutant proteins. Series begin at anaphase onset. Scale bar, 10 μm. (**C**) Graphs showing the kinetics of contractile ring closure in individual embryos for the conditions shown in (B). Star in bottom right graph marks the final furrow width before regression. (**D**) Graph plots percent embryonic lethality (mean ± SD) after depletion of endogenous ECT-2 for embryos expressing the indicated WT or the ECT-2 Basic Surface mutant proteins 3A and 3E from RNAi-resistant transgenes. N is number of worms; n is the number of embryos scored per condition. (**E**) Graphs showing the kinetics of contractile ring closure in individual embryos for the indicated conditions. Combining the CYK-4 4A and ECT-2 Basic Surface 3A mutations in embryos expressing the ECT-2 activator NOP-1 results in a phenotype similar to the ECT-2 Basic Surface 3A mutant alone. Stars mark the final furrow width before regression. (**F**) Single central plane confocal images of the cell equator from time-lapse sequences of embryos expressing ZEN-4::mScarlet in which CYK-4 is reconstituted with transgenic WT CYK-4. In the top sequence SPD-1 is present and the central spindle is intact (n=10). In the bottom sequence, SPD-1 is depleted and the central spindle is disrupted as indicated in the schematics (n=11). Series begin at furrow initiation. Scale bar, 10 μm.

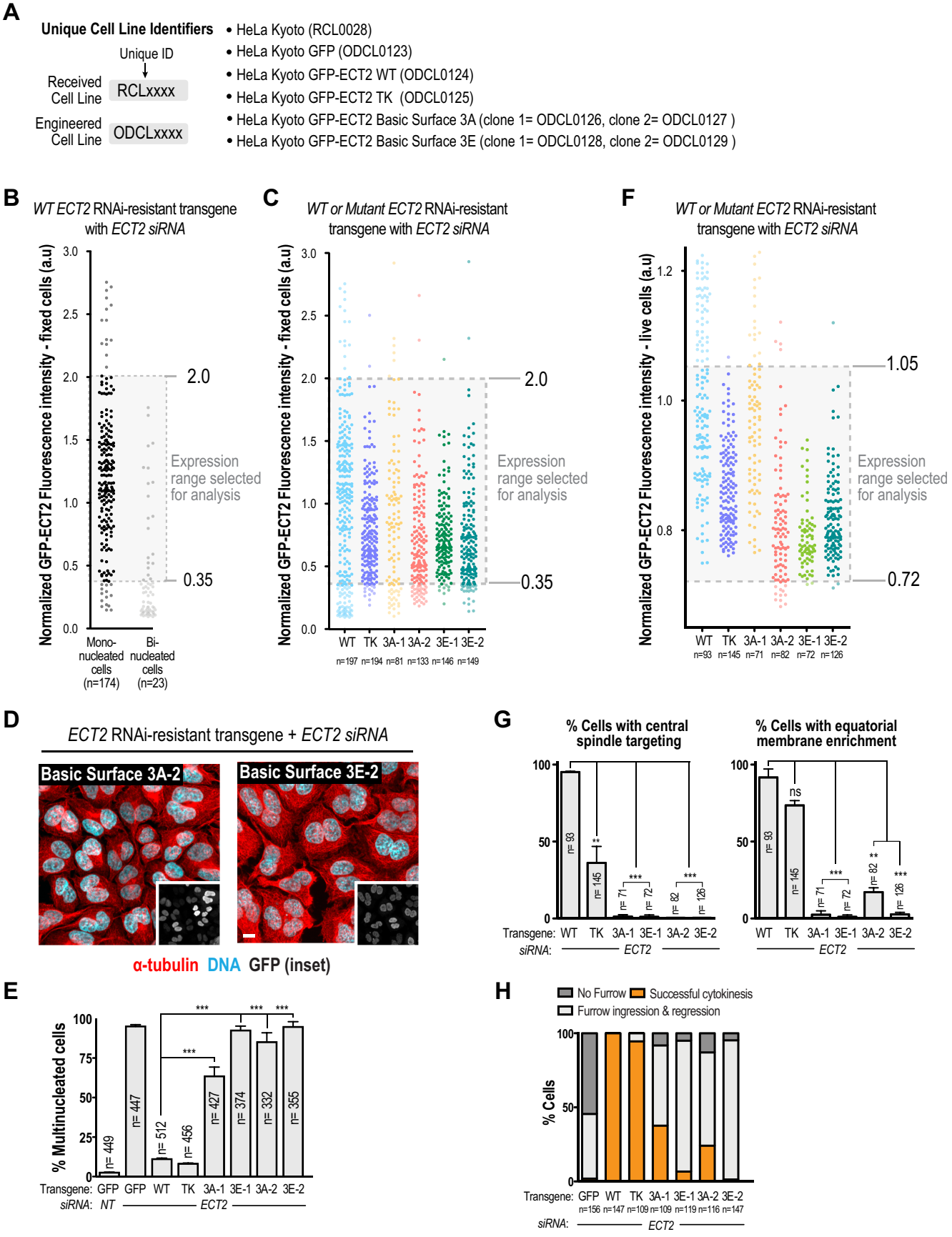
A
Unique Cell Line Identifiers
Unique ID
Received Cell Line
RCLxxxx
Engineered Cell Line
ODCLxxxx
• HeLa Kyoto (RCL0028)
• HeLa Kyoto GFP (ODCL0123)
• HeLa Kyoto GFP-ECT2 WT (ODCL0124)
• HeLa Kyoto GFP-ECT2 TK (ODCL0125)
• HeLa Kyoto GFP-ECT2 Basic Surface 3A (clone 1= ODCL0126, clone 2= ODCL0127)
• HeLa Kyoto GFP-ECT2 Basic Surface 3E (clone 1= ODCL0128, clone 2= ODCL0129)
B
WT ECT2 RNAi-resistant transgene with ECT2 siRNA
Normalized GFP-ECT2 Fluorescence intensity - fixed cells (a.u)
2.0
0.35
Expression range selected for analysis
Mono-nucleated cells (n=174)
Bi-nucleated cells (n=23)
C
WT or Mutant ECT2 RNAi-resistant transgene with ECT2 siRNA
Normalized GFP-ECT2 Fluorescence intensity - fixed cells (a.u)
2.0
0.35
Expression range selected for analysis
WT TK 3A-1 3A-2 3E-1 3E-2
n=197 n=194 n=81 n=133 n=146 n=149
F
WT or Mutant ECT2 RNAi-resistant transgene with ECT2 siRNA
Normalized GFP-ECT2 Fluorescence intensity - live cells (a.u)
1.05
0.72
Expression range selected for analysis
WT TK 3A-1 3A-2 3E-1 3E-2
n=93 n=145 n=71 n=82 n=72 n=126
D
ECT2 RNAi-resistant transgene + ECT2 siRNA
Basic Surface 3A-2
Basic Surface 3E-2
α-tubulin DNA GFP (inset)
G
% Cells with central spindle targeting
% Cells with equatorial membrane enrichment
Transgene: WT TK 3A-1 3E-1 3A-2 3E-2
siRNA: ECT2
ns
E
% Multinucleated cells
n= 449
n= 447
n= 512
n= 456
n= 427
n= 374
n= 332
n= 355
Transgene: GFP GFP WT TK 3A-1 3E-1 3A-2 3E-2
siRNA: NT ECT2
H
No Furrow
Successful cytokinesis
Furrow ingression & regression
% Cells
Transgene: GFP WT TK 3A-1 3E-1 3A-2 3E-2
n=156 n=147 n=109 n=109 n=119 n=116 n=147
siRNA: ECT2

Figure S7. Mutation of the conserved basic surface in the BRCT-1 module of ECT2 results in consistent phenotypes across different independent clones, Related to Figure 6. (**A**) (*left*) Unique cell line identifiers are used to describe human cell lines. The RCL prefix refers to cell lines received from an external source. The ODCL prefix refers to cell lines engineered from received cell lines. (*right*) The codes for each of the clonal HeLa Kyoto cell lines generated for this study are listed. (**B**) Graph plotting total nuclear GFP-ECT2 fluorescence intensity of fixed cells that were mono- or bi-nucleated after 48 hours of endogenous ECT2 depletion. This analysis was used to define the range of WT GFP-ECT2 intensities sufficient to support cytokinesis (*gray box*). For comparative analysis of the clonal cell lines expressing GFP-ECT2 fusions, only cells with nuclear GFP-ECT2 intensities within the protective range defined by WT GFP-ECT2 were analyzed for multi-nucleation after endogenous ECT2 depletion. (**C**) Representative graph for one of the three experiments performed plotting total GFP nuclear fluorescence intensity for cells from the indicated cell lines after endogenous ECT2 depletion. Gray box indicates cells that were analyzed to measure the multinucleation frequency. (**D**) Representative images of fields of cells expressing the indicated GFP-ECT2 fusions after depletion of the endogenous protein by transfection with *ECT2* siRNA. Scale bar, 10μm. (**E**) Graph plotting the percentage of multinucleated cells from the experiments in Figure 6C and Figure S7D (mean ± SE). Bars represent mean values of three independent experiments. n represents the total number of cells scored for each condition. On average, 150 cells were scored for each experiment. Data is the same as in Figure 6D with data for two additional clones (3A-2 and 3E-2) added. (**F**) Graph plotting total GFP nuclear fluorescence intensity in living cells from the indicated cell lines after endogenous depletion of ECT2. Gray box marks the cells from each line that were scored for spindle midzone targeting and equatorial membrane enrichment. (**G**) Graph plotting the percentage of cells in which the indicated WT or mutant GFP-ECT2 fusions localized to the central spindle (*left graph*) or were enriched on the equatorial membrane (*right graph*) after depletion of endogenous ECT2. Bars represent mean values of two independent experiments; error bars are the SE. n represents the total number of cells scored for each condition. Data is the same as in Figure 6I with data for two additional clones (3A-2 and 3E-2) added. (**H**) Quantification of cytokinetic phenotypes scored between 24 and 48 hours after siRNA transfection. Data is the same as in Figure 6J with data for two additional clones (3A-2 and 3E-2) added.

CYK-4					
Cluster	**#**	**Sequence**	**Conserved?**	**Score**	**Consensus?**
I	3	*****MKSSTSKEKV	Yes	1.815	No
	4	****MKSSTSKEKVC	Yes	2.442	No
	6	**MKSSTSKEKVCGE	Yes	1.837	No
	15	EKVCGENSRHIFNMI	Yes	2.703	No
	57	LWKDSEESKKRLNAD	Yes	3.659	No
	89	FDIDVKDTQKHLRAL	Yes	1.359	No
II	163	HPHLMEDTQDDEDDS	Yes	2.678	Yes
	170	TQDDEDDSEVDYDET	No	4.225	Yes
	177	SEVDYDETGDSFEEV	Yes	2.475	Yes
	180	DYDETGDSFEEVIHL	Yes	2.033	No
III	209	AVGGKRRSASAHAIT	Yes	1.895	No
	211	GGKRRSASAHAITAA	Yes	1.261	No
	224	AAANSKRSRSRVMTA	Yes	1.833	No
	226	ANSKRSRSRVMTATI	Yes	1.62	No
	232	RSRVMTATIDEEPNE	Yes	1.928	No
IV	259	STPHQEMTTTTTTTT	Yes	1.572	No
	268	TTTTTTTTTIHNSRA	Yes	1.312	No
	269	TTTTTTTTIHNSRAQ	Yes	1.322	No
	273	TTTTIHNSRAQNQDP	Yes	1.264	No
V	293	HRQLTRRSLSCGSIP	Yes	2.076	No
	298	RRSLSCGSIPSCDQT	Yes	1.286	No
	325	SSAILTKSTLDIRTL	Yes	1.217	No
	326	SAILTKSTLDIRTLK	Yes	1.428	No
VI	587	MGHPVKQSQSQAIAG	Yes	1.482	No
	589	HPVKQSQSQAIAGRD	Yes	1.246	No
	622	WQRFLGTSAVSMASN	Yes	1.953	No
	646	NFALCDRSILGPVTT	Yes	3.283	Yes

ECT-2					
Cluster	**#**	**Sequence**	**Conservation?**	**Score**	**Consensus?**
I	4	****MDVSMLQSPQK	Yes	5.866	Yes
	64	SGDWSEYTFFCGNFD	Yes	1.565	Yes
II	323	LRSQNSRSLSSMRDC	Yes	3.047	No
	325	SQNSRSLSSMRDCSV	Yes	2.558	No
	896	NILGRNTSMRRQATG	Yes	1.75	Yes
III	123	CELMKDVTMKLAAEV	Yes	2.558	Yes
	331	LSSMRDCSVEGPTSL	Yes	5.406	Yes
IV	380*	ETEKNYLSLLKLVVK	Yes	0.812	Yes
	478	QYINSYDTIKRLFDK	Yes	1.228	Yes
	791	TEWSHNESFMPPPQS	Yes	3.264	Yes
V	171	EAKVQSISLVGVPTM	Yes	1.649	No
	236	MLRSLENTGGKLAPS	Yes	1.533	No

	315	VSSPIGKSLRSQNSR	Yes	2.768	No
	362	CKSPRQPSKRLRVCM	Yes	1.652	No
VI	405	HNEFMSRSDVAMMFG	Yes	1.551	No
	491	DKQDRENSKFHTFCK	Yes	2.366	No
VII	787	QMNITEWSHNESFMP	Yes	2.116	No
	836	GQINENTTFLQSPRV	Yes	2.406	Yes
	866	LPGCQSESESTPKRG	Yes	1.975	No
	869	CQSESESTPKRGIRS	Yes	2.185	No
VIII	917	ELPRSKTSSYRVTDI	Yes	2.062	No
	918	LPRSKTSSYRVTDI*	Yes	2.279	No
	922	KTSSYRVTDI*****	Yes	1.678	No
IX	310	LESSSVSSPIGKSLR	Yes	1.348	No
	315	VSSPIGKSLRSQNSR	Yes	2.768	No
	318*	PIGKSLRSQNSRSLS	No	0.848	No
	321	KSLRSQNSRSLSSMR	Yes	2.504	No
	323	LRSQNSRSLSSMRDC	Yes	3.047	No
	325	SQNSRSLSSMRDCSV	Yes	2.558	No
	326	QNSRSLSSMRDCSVE	Yes	1.391	No
	331	LSSMRDCSVEGPTSL	Yes	5.406	Yes
	362	CKSPRQPSKRLRVCM	Yes	1.652	No

* Site does not meet score cutoff but was included due to conservation or proximity to a selected site.

ZEN-4					
Cluster	**#**	**Sequence**	**Conserved?**	**Score**	**Consensus?**
I	2	******MSSRKRGIT	Yes	1.83	No
	21	QVRRKKLSIEETDSI	Yes	2.446	No
	25	KKLSIEETDSIEVVC	Yes	1.536	No
	92	QATVFERTSVDLILN	No	2.145	No
	93	ATVFERTSVDLILNL	Yes	1.772	No
II	51	LIAIDEGSIQTVLPP	Yes	3.522	Yes
	93	ATVFERTSVDLILNL	Yes	1.772	No
	106	NLLKGQNSLLFTYGV	Yes	1.638	No
	157*	EKCIFYPSALNTFEI	No	0.42	Yes
	189	LSTSREITDRYCEAI	Yes	1.511	No
III	189	LSTSREITDRYCEAI	Yes	1.511	No
	257	GAKDVEVSSSEEALE	Yes	2.862	No
	259	KDVEVSSSEEALEVF	Yes	2.29	No
	278	ERRRVSSTLLNKDSS	Yes	1.819	No
	284	STLLNKDSSRSHSVF	Yes	1.674	No
	285	TLLNKDSSRSHSVFT	Yes	2.21	No
	289	KDSSRSHSVFTIKLV	Yes	2.279	No
IV	310*	ETKSVYPTMDSSQII	No	0.457	Yes
	314	VYPTMDSSQIIVSQL	Yes	2.967	No
	347	ERLAEANSINQSLMT	Yes	1.583	No

	351	EANSINQSLMTLRQC	Yes	3.319	Yes
	368	VLRRNQKSSSQNLEQ	Yes	2.21	No
	369	LRRNQKSSSQNLEQV	No	1.565	No
	370	RRNQKSSSQNLEQVP	No	2.04	No
V	415	DDYDENMSALAFAEE	Yes	2.899	Yes
	423	ALAFAEESQTIEVKK	Yes	3.978	No
	425	AFAEESQTIEVKKQV	No	2.091	No
	455	WNSELDGSVRMEDDG	No	3.29	Yes
VI	494	YKYARKLSSLQNSSE	No	2.913	No
	495	KYARKLSSLQNSSEE	No	1.569	No
	499	KLSSLQNSSEEGPSS	Yes	2.587	No
	500	LSSLQNSSEEGPSST	Yes	3.054	No
	507	SEEGPSSTLLTMIRQ	No	1.964	No
	532	EIARLKDSLNDKDEE	No	2.594	No
	556	RYKRENASMKERIAS	No	2.533	Yes
VII	499	KLSSLQNSSEEGPSS	Yes	2.587	No
	500	LSSLQNSSEEGPSST	Yes	3.054	No
	607	RGIIDNPSPSVASLR	Yes	1.58	No
	609	IIDNPSPSVASLRSR	Yes	2.562	No
VIII	652	FKKRLEATTSTTVMS	No	2.333	No
	656	LEATTSTTVMSGSSS	No	2.464	No
	661	STTVMSGSSSGGSGQ	No	2.094	No
	723	EMHQLNKSGEYRLTH	No	1.844	No
	740	VDDEGNISTNIVKGN	Yes	1.453	No
	770	IERLTHESPSTRK**	Yes	1.667	No

* Site does not meet score cutoff but was included due to conservation or proximity to a selected site.

Table S1. Putative PLK-1 phosphorylation sites in CYK-4, ECT-2 and ZEN-4, Related to Figure 2.

SUPPLEMENTAL REFERENCE

S1. Woodruff, J.B., Wueseke, O., Viscardi, V., Mahamid, J., Ochoa, S.D., Bunkenborg, J., Widlund, P.O., Pozniakovsky, A., Zanin, E., Bahmanyar, S., et al. (2015). Centrosomes. Regulated assembly of a supramolecular centrosome scaffold in vitro. Science *348*, 808-812.